HHS Public Access

Author manuscript

J Invest Dermatol. Author manuscript; available in PMC 2022 December 30.

Published in final edited form as:

J Invest Dermatol. 2022 May ; 142(5): 1243–1252.e1. doi:10.1016/j.jid.2022.01.016.

Research Techniques Made Simple: Emerging Imaging Technologies for Noninvasive Optical Biopsy of Human Skin

Griffin Lentsch[1], **Erica G. Baugh**[2], **Bonnie Lee**[2], **Michelle Aszterbaum**[2], **Christopher B. Zachary**[2], **Kristen M. Kelly**[1,2], **Mihaela Balu**[1]

[1]Beckman Laser Institute and Medical Clinic, University of California, Irvine, California, USA

[2]Department of Dermatology, University of California, Irvine, California, USA

Abstract

Over the past few years, high-resolution optical imaging technologies such as optical coherence tomography (OCT), reflectance confocal microscopy (RCM), and multiphoton microscopy (MPM) have advanced significantly as new methodologies for clinical research and for real-time detection, diagnosis, and therapy monitoring of skin diseases. Implementation of these technologies into clinical research and practice requires clinicians to have an understanding of their capabilities, benefits, and limitations. This concise review provides insights on the application of OCT, RCM, and MPM for clinical skin imaging through images acquired in vivo from the same lesions. The presented data are limited to pigmented lesions and basal cell carcinoma.

Introduction

In the field of dermatology, there are several optical imaging technologies currently applied for noninvasive subsurface skin imaging as identified by Tkaczyk (2017) in a recent comprehensive review. Among these techniques, optical coherence tomography (OCT), reflectance confocal microscopy (RCM), and multiphoton microscopy (MPM) distinguish themselves on the basis of spatial resolution that ranges from a few microns (OCT) to submicron (MPM). The potential of RCM and MPM for noninvasive clinical skin imaging

Correspondence: Mihaela Balu, Beckman Laser Institute and Medical Clinic, University of California, 1002 Health Sciences Road., Irvine, California 92617, USA. mbalu@uci.edu.

AUTHOR CONTRIBUTIONS

Conceptualization: MB, CBZ, KMK; Formal analysis: GL, MB, BL, EGB, MA; Methodology: GL MB; Resources: MB, MA, CBZ, KMK; Supervision: MB, KMK; Writing - Original Draft Preparation: MB, GL; Writing - Review and Editing: MB, EGB, BL, CBZ, KMK, MA

CONFLICT OF INTEREST

MB is coauthor of a patent owned by the University of California, Irvine (Irvine, CA), which is related to multiphoton microscopy (MPM) imaging technology. MB and CBZ are cofounders of Infraderm, LLC, a startup spin off from the University of California, Irvine, which develops MPM-based clinical imaging platforms for commercialization purposes. The Institutional Review Board and Conflict of Interest Office of the University of California, Irvine, have reviewed patent disclosures and did not find any concerns. Neither of the authors have any financial interest in any entities that commercialize the imaging devices described in this manuscript.

SUPPLEMENTARY MATERIAL

Supplementary material is linked to the online version of the paper at www.jidonline.org, and at https://doi.org/10.1016/j.jid.2022.01.016.

has been shown for a broad range of applications from noninvasive diagnostics (Balu et al., 2014; Nwaneshiudu et al., 2012; Pezzini et al., 2020) and monitoring treatment (Balu et al., 2017; Malvehy et al., 2016) to clinical and cosmetic research (Tancrède-Bohin et al., 2020). OCT has been shown to be of value in the noninvasive diagnosis of nonmelanoma skin cancer (Que, 2016) and in skin diseases related to dynamic changes in vasculature (Olsen et al., 2018). Clinical skin imaging devices based on these technologies have been commercially available for some time (>10 years for MPM and OCT; >20 years for RCM). Yet, few dermatologists are familiar with RCM imaging of the skin, and even fewer are familiar with OCT and MPM.

This concise review provides insights on the application of OCT, RCM, and MPM for clinical skin imaging and describes a comparison of their benefits and limitations related to various skin conditions.

OCT, RCM, MPM: technology background and current commercial devices for clinical skin imaging

OCT.

This is an interferometric optical imaging technique that can generate three-dimensional (3D) images of tissue microstructures by measuring backscattered and back-reflected light in a way that is analogous to ultrasound, using light rather than sound as a light source (Huang et al., 1991). This results in improved resolution for OCT (1–2 orders of magnitude higher than conventional ultrasound) but also in limited penetration depth (about 2–3 mm in most tissues, about 1 mm in the skin) when compared with that for ultrasound imaging (Fujimoto et al., 2000). OCT has also the ability to detect particle motion corresponding to blood flow and thus reveal the morphology of the blood vessels structure in the imaged volume. It is used in a wide range of research and clinical applications, with the largest clinical impact in ophthalmology. Recent technical advances that improved lateral and depth resolutions have broadened the range of applications for OCT imaging to include dermatology. OCT recently received category III Current Procedural Terminology (CPT) codes from the American Medical Association, enabling tracking of its use in the medical community. Currently, there are two OCT-based systems that hold a medical CE mark and are cleared by the US Food and Drug Administration (FDA) as a 510(k) device for skin imaging: the Skintell (Agfahealthcare, Mortsel, Belgium) and VivoSight developed by Michelson Diagnostics (Orpington, United Kingdom). The latter is used in this study (Figure 1a). To facilitate the VivoSight integration in clinical practice, Michelson Diagnostics offers a range of educational events (seminars, workshops, seminars) along with several training resources available online (Vivosight).

RCM.

This is an optical imaging technique that provides subcellular resolution images on the basis of differences in the refractive indices of tissue components. It uses near-infrared light from a diode laser as the excitation source. The focused laser light is raster scanned on the skin surface, and the backscattered light is collected to provide gray-scale images on reconstruction. The 3D images of the skin, commonly known as z-stacks, are obtained by

moving the focusing lens in the z-direction, thus scanning at different depths in the skin. The development of the RCM-based laser scanning tomograph by Lucid (currently Caliber I.D., Rochester, NY) marked the advance of this technology into the clinical setting, prompting a wide range of imaging applications in dermatology in the last 20 years (Levine and Markowitz, 2018). The clinical RCM device used in this study is VivaScope 1500 (Figure 1b) developed by Caliber I.D., currently in the process of merging with MAVIG GmbH (München, Germany). It has CE mark, FDA (510k) clearance, and six category I CPT reimbursement codes, unique descriptors for well-defined procedures, unlike the category III CPT temporary codes assigned to emerging technologies and procedures. The Center for Medicare and Medicaid Services has valued all the six of these RCM codes for Medicare/Medicaid coverage (Levine and Markowitz, 2018). RCM provides higher spatial resolution than OCT but limited penetration depth (up to 200–250 μm) and limited field of view (FOV). The FOV provided by the VivaScope 1500 has been extended by implementation of a mosaic tiling feature (acquisition of adjacent FOVs) that allows areas up to 8 × 8 mm^2 to be imaged. Caliber I.D. offers a comprehensive training program through on-site and online training, expert tutorials, video lectures, and workshops (Confocal Training). The International Confocal Group offers the opportunity to join a group of over 100 physicians involved in education, investigation, and collaboration programs related to using RCM in clinical practice (International Confocal Group).

MPM.

This is also a laser scanning microscopy technique with a contrast mechanism different from that of RCM. In the skin, MPM contrast is derived from second harmonic generation (SHG) of collagen and two-photon excited fluorescence (TPEF) of autofluorescent species such as the cofactors reduced nicotinamide adenine dinucleotidec and flavin adenine dinucleotide, elastin, keratin, and melanin. Owing to the different contrast mechanisms, MPM images can be multicolor and can distinguish cellular features from the extracellular matrix. This contrast closely resembles the histologic sections dermatopathologists use for diagnosis. MPM is a more complex imaging technology than RCM and OCT. Its clinical translation has been challenging mainly owing to the large footprints of the ultrafast laser sources; the lack of a stable, flexible patient interface; and blurring effects due to physiological motion artifacts caused by the relatively slow scanning. These challenges have been successfully overcome with the development of a portable, clinical multiphoton tomograph, MPTflex (Figure 1c), by Jenlab, GmbH (Jena, Germany). The imaging platform uses a Ti:Sapphire as a light source, and it features an articulated arm to allow for imaging of almost any region of the body. It is CE marked for clinical use. In the United States, it is currently employed exclusively for clinical research. Because the MPTflex is primarily used in a limited number of locations for clinical research, there are limited resources for training and tutorials related to image interpretation and analysis. In the United States, video lectures and hands-on training on using the MPTflex are available at the Beckman Laser Institute and Medical Clinic (Irvine, CA) during the yearly workshop offered by the Laboratory of Fluorescence Dynamics at the University of California Irvine (Irvine, CA) (Laboratory for Fluorescence Dynamics).

Previous Research Techniques Made Simple articles describe in more detail the basic principles of OCT (Que, 2016), RCM (Nwaneshiudu et al., 2012; Que, 2016), and MPM (Obeidy et al., 2018) in the context of skin imaging.

Table 1 presents a summary of the key parameters related to the images generated with each of the commercial devices (Figure 1) on the basis of the three technologies: OCT, RCM, and MPM. Similar devices may be under development and commercialized by other manufacturers.

RCM, MPM, OCT imaging: Clinical value

All images presented in this review were acquired in vivo from patients with normal and lesional skin using the devices presented in Figure 1. All measurements were conducted according to an approved institutional review board protocol of the University of California, Irvine (HS#2008-6307), with written informed consent obtained from all patients. The volumetric images acquired over mm-scale skin areas by the VivoSight (OCT) and the VivaScope (RCM) encompassed the smaller scale volume sampled by the MPTflex (MPM). Thus, the appearance of the same morphological features can be compared side by side in the images provided by all the three technologies.

Normal skin as visualized by OCT, RCM, and MPM.

Representative OCT, RCM, and MPM images acquired from the forearm of a volunteer are presented in Figure 2. The OCT image (Figure 2b), generated as a vertical (x–z) optical section, shows the stratum corneum as a hyperreflective layer on the skin top surface and the dermal–epidermal junction (DEJ) as a hyporeflective contour that separates the epidermis from the dermis. OCT also captures the morphology of the dermal vasculature. RCM and MPM images are generally acquired as horizontal (x–y) optical sections at different depths from the stratum corneum to the superficial dermis. The single-depth images presented in Figure 2 underscore the ability of RCM to generate images of mm-scale tissue areas, whereas MPM samples a significantly smaller tissue area but with enhanced contrast, allowing for the detection of collagen starting at the DEJ, among other molecular components.

The depth-resolved morphology of a volunteer’s forearm normal skin as visualized by RCM and MPM is presented in Figure 3. The keratinocytes (KCs) of the granulosum and spinosum layers have a slightly different appearance in the MPM and RCM images owing to the different origin of signals, but both techniques visualize them as bright cells with dark nuclei. The KCs of the basal layer have a more similar appearance in the MPM and RCM images, particularly when they are pigmented and display the bright melanin caps. Depending on the depth along the DEJ, the KCs of the basal layer appear either as bright cells arranged in clusters or in a circular pattern surrounding the dermal papilla. This pattern has enhanced contrast in African-Americans and other highly pigmented skin compared with that in Caucasian lighter skin types, allowing for better visualization of certain morphologies; however, the lighter skin allows for imaging penetration through deeper dermis than darker skin. Collagen and elastin fibers are selectively detected by

MPM on the basis of their SHG and TPEF signals, respectively. RCM does not distinguish collagen from elastin fibers.

Basal cell carcinoma as visualized by OCT, RCM, and MPM.

Basal cell carcinoma (BCC) is a form of skin cancer that originates from the basal cells of the epidermis and associated follicular structures. Histopathologically, it is characterized by the presence in the dermis and/or at the DEJ of islands of basaloid cells, often showing palisading in the peripheral cell layer. The morphological features of a BCC lesion on the upper arm of a patient, as captured noninvasively by OCT, RCM, and MPM, are illustrated in Figure 4. The OCT captured the vasculature around the lesion and the nests of basaloid cells, imaged as bright islands delineated by dark rims. The BCC nests are more clearly outlined by surrounding collagen in the RCM images and generally present as a well-resolved cellular structure in the MPM images, particularly for superficial BCC types.

Melanocytic nevi as visualized by OCT, RCM, and MPM.

Figure 5 presents representative OCT, RCM, and MPM images acquired in vivo from a melanocytic nevus of a patient's arm. After excision, on the basis of histopathology, the lesion was diagnosed as a benign dermal nevus. Volumetric images were acquired with all the three techniques; nonetheless, single x–z (OCT) and x–y (RCM, MPM) images at a particular depth are shown for easier visualization of the features. The depth of the lesion is clearly delineated in the OCT image along with the vasculature around the lesion; however, the morphological features specific to a melanocytic nevus are not distinguished owing to the limited spatial resolution of OCT. Well-defined nests of nevus cells are captured by both RCM and MPM. The RCM provides enhanced information about the overall morphology of the lesion by imaging an mm-scale area, whereas MPM better resolves the cellular structures within the nests and the surrounding collagen fibers.

Recurrence of melanocytic nevi can occur after incomplete removal and can resemble melanoma both histologically and clinically. Histologically, they are commonly characterized by an irregular proliferation of atypical melanocytes, dermal fibrosis, and an inflammatory infiltrate. Generally, these morphological features are well-captured by RCM and MPM as illustrated by the images in Figure 6 acquired in vivo from a recurrent compound melanocytic nevus on the hand of a patient. Although the dendritic and inflammatory cells are imaged with comparable contrast by both MPM and RCM, the morphological information is captured by RCM over much larger depth-resolved tissue areas. However, the dermal morphology around the inflammatory infiltrate is better identified by MPM owing to the SHG-based contrast that allows for visualization of collagen fibers. The presence of inflammation makes the delineation of the lesion depth more challenging with OCT imaging than that of dermal nevus previously discussed. In addition, the dendritic and inflammatory cells are not distinguished by OCT owing to the limited spatial resolution.

Spitz nevus is a benign melanocytic nevus with histologic features that overlap with those of melanoma. Characteristic morphological features such as occasional upward migration of dendritic cells in the center of the lesion and large junctional nests of spindle dendritic

cells are well captured in vivo by both MPM and RCM, as illustrated in the images of Figure 7 acquired from a lesion on the forearm of a patient histologically diagnosed as a residual/recurrent nevus originally diagnosed as a Spitz nevus. Dendritic cells are imaged by both MPM and RCM, whereas the melanocytic nests and their dermal location are more clearly distinguished in the MPM images on the basis of the selective detection of collagen fibers. The depth-resolved RCM mosaic images allow for the morphology assessment at mm scale with microscopic resolution. The limited spatial resolution of OCT does not allow for the clear delineation of the lesion or its microscopic morphology.

Melanoma as visualized by OCT, RCM, and MPM.

Melanoma is one of the deadliest forms of skin cancers that would considerably benefit from early, noninvasive diagnosis. The most common standard-of-care histologic diagnostic criteria for melanoma include pagetoid spread, atypical melanocytes, architectural disorder at the DEJ, and invasion of tumor cells into the dermis (Navarrete-Dechent et al., 2021). Figure 8 presents representative images acquired in vivo by OCT, RCM, and MPM from a skin lesion on a patient's upper arm, histologically diagnosed as invasive melanoma. The spatial resolution of RCM and MPM allows for visualization of pagetoid spread (Figure 8 e1 and e2 and f1 and f2), epidermal disarray (Figure 8 e1–e5 and f1–f5), and nests of melanoma cells at the DEJ (Figure 8 e5 and f5). As described for the previous lesions, the RCM mosaic imaging captures the overall morphology of the lesion with microscopic resolution, whereas the DEJ and the location of the melanoma nests are more clearly identified in the MPM images on the basis of the molecular contrast provided by this imaging approach. The OCT image reveals a raised lesion with an increased density of blood vessels.

Benefits and limitations

The main advantage of OCT, RCM, and MPM over other imaging technologies is the ability to provide noninvasive depth-resolved images (optical biopsy) beneath the skin surface with a few microns (OCT), micron (RCM), or submicron (MPM) spatial resolution. OCT presents images with the lowest spatial resolution among the three imaging approaches, but it samples a larger volume than RCM and MPM. It also provides functionality in addition to structural information, allowing for the assessment of changes in the vasculature network in the skin. On the basis of these abilities, OCT has shown potential for the noninvasive diagnosis and delineation of nonmelanoma skin cancer (Sinx et al., 2020), the evaluation of alopecia (Ekelem et al., 2021), and noninvasive diagnosis and delineation of skin diseases related to dynamic changes in the vasculature (Olsen et al., 2018). RCM has a superior spatial resolution to OCT, and therefore it has been evaluated and proved an efficient imaging approach in dermatology for a broader range of applications such as noninvasive diagnosis of melanoma (Pezzini et al., 2020; Yélamos et al., 2017), nonmelanoma skin cancer (Que, 2016), and other skin conditions (Levine and Markowitz, 2018); monitoring of skin therapy (Malvehy et al., 2016); or evaluation of human skin microcirculation (Saknite et al., 2020). The major limitation of RCM is related to its contrast mechanism that provides grayscale images requiring extensive training to achieve accurate image interpretation. MPM offers molecular contrast on the basis of endogenous signals

from different molecular components in the skin, which results in multicolor images that distinguish cellular features from the extracellular matrix facilitating image interpretation, implementation of quantitative image analysis approaches (Balu et al., 2014; Lentsch et al., 2020, 2019; Lin et al., 2019), and evaluation of skin aging based on selective detection of collagen and elastin fibers (Puschmann et al., 2012). In addition, the detection of the reduced nicotinamide adenine dinucleotidec based on its fluorescence intensity and lifetime allows for the assessment of metabolic changes related to a variety of skin conditions, including skin carcinogenesis (König, 2020; Pouli et al., 2016). The main limitation of MPM as integrated into the current commercial device is the small FOV, which affects the accuracy of the overall assessment of lesions, particularly for nonuniform pigmented lesions such as melanoma arising in nevi. MPM has also a significantly slower scanning rate than OCT and RCM. Both MPM and RCM have limited penetration depth compared with OCT. Nonetheless, they have the ability to capture the DEJ and the superficial dermis where many underlying skin conditions originate, including skin cancer. Overall, all these technologies have benefits and limitations to consider before selecting the appropriate device for a specific application. Many clinical applications may require a multimodality approach that incorporates more than one of these imaging tools (Koehler et al., 2011; Monnier et al., 2021; Sahu et al., 2018).

Moving forward

Addressing the current technical challenges is essential for improving clinical access and the adoption of these technologies. There are continuous efforts to improve the spatial resolution of OCT (Dubois et al., 2018; Wang et al., 2021), the RCM contrast (Campanella et al., 2022), the FOV and imaging speed of MPM (Fast et al., 2020) as well as its penetration depth (Balu et al., 2015), and the MPM instrument compactness and portability (Fast et al., 2020; König et al., 2021). Ultimately, overcoming the technical and practical challenges related to the translation of these imaging technologies to clinical practice requires close collaboration among engineers, scientists, and clinicians to identify needs and the right approach to address them.

ACKNOWLEDGMENT

The authors would like to thank Jenlab GmbH, Caliber I.D., and Michelson Diagnostics for lending the imaging devices used in this study. MB acknowledges the grant support from the National Institute of Biomedical Imaging and Bioengineering (R01EB026705) and from the Skin Biology Resource-Based Center, University of California, Irvine (Irvine, CA) (P30AR075047).

Abbreviations:

3D	three-dimensional
BCC	basal cell carcinoma
CPT	Current Procedural Terminology
DEJ	dermal–epidermal junction
FDA	Food and Drug Administration

FOV	field of view
KC	keratinocyte
MPM	multiphoton microscopy
OCT	optical coherence tomography
RCM	reflectance confocal microscopy
SHG	second harmonic generation
TPEF	two-photon excited fluorescence

REFERENCES

Balu M, Kelly KM, Zachary CB, Harris RM, Krasieva TB, König K, et al. Distinguishing between benign and malignant melanocytic nevi by in vivo multiphoton microscopy. Cancer Res 2014;74:2688–97. [PubMed: 24686168]

Balu M, Lentsch G, Korta DZ, König K, Kelly KM, Tromberg BJ, et al. In vivo multiphoton-microscopy of picosecond-laser-induced optical breakdown in human skin. Lasers Surg Med 2017;49:555–62. [PubMed: 28333369]

Balu M, Saytashev I, Hou J, Dantus M, Tromberg BJ. Sub-40 fs, 1060-nm Yb-fiber laser enhances penetration depth in nonlinear optical microscopy of human skin. J Biomed Opt 2015;20:120501. [PubMed: 26641198]

Campanella G, Navarrete-Dechent C, Liopyris K, Monnier J, Aleissa S, Minhas B, et al. Deep learning for basal cell carcinoma detection for reflectance confocal microscopy. J Invest Dermatol 2022;142:97–103. [PubMed: 34265329]

Confocal Training. RCM training, https://www.confocaltraining.com/training/; (accessed 19 October 2021).

Dubois A, Levecq O, Azimani H, Siret D, Barut A, Suppa M, et al. Line-field confocal optical coherence tomography for high-resolution noninvasive imaging of skin tumors. J Biomed Opt 2018;23:1–9.

Ekelem C, Feil N, Csuka E, Juhasz M, Lin J, Choi F, et al. Optical coherence tomography in the evaluation of the scalp and hair: common features and clinical utility. Lasers Surg Med 2021;53:129–40. [PubMed: 32253781]

Fast A, Lal A, Durkin AF, Lentsch G, Harris RM, Zachary CB, et al. Fast, large area multiphoton exoscope (FLAME) for macroscopic imaging with microscopic resolution of human skin. Sci Rep 2020;10:18093. [PubMed: 33093610]

Fujimoto JG, Pitris C, Boppart SA, Brezinski ME. Optical coherence tomography: an emerging technology for biomedical imaging and optical biopsy. Neoplasia 2000;2:9–25. [PubMed: 10933065]

Huang D, Swanson EA, Lin CP, Schuman JS, Stinson WG, Chang W, et al. Optical coherence tomography. Science 1991;254:1178–81. [PubMed: 1957169]

International Confocal Group. http://www.confocal-icwg.com/; (accessed 19 October 2021).

Koehler MJ, Speicher M, Lange-Asschenfeldt S, Stockfleth E, Metz S, Elsner P, et al. Clinical application of multiphoton tomography in combination with confocal laser scanning microscopy for in vivo evaluation of skin diseases. Exp Dermatol 2011;20:589–94. [PubMed: 21539618]

König K Review: clinical in vivo multiphoton FLIM tomography. Methods Appl Fluoresc 2020;8:034002. [PubMed: 32320386]

König K, Pankin D, Paudel A, Hänßle H, Winkler J, Zieger M, et al. Skin cancer detection with a compact multimodal fiber laser multiphoton FLIM tomograph. In: Pariasamy A, So PTC, König K, editors. Prooceedings volume 11648: multiphoton microscopy in the biomedical sciences. SPIE BIOS; 2021. p. 1164801–8.

Laboratory for Fluorescence Dynamics. 15th LFD Workshop in Advanced Fluorescence Imaging and Dynamics. https://www.lfd.uci.edu/workshop/; 2021 (accessed October 19, 2021).

Lentsch G, Balu M, Williams J, Lee S, Harris RM, König K, et al. In vivo multiphoton microscopy of melasma. Pigment Cell Melanoma Res 2019;32:403–11. [PubMed: 30506627]

Lentsch G, Valdebran M, Saknite I, Smith J, Linden KG, König K, et al. Noninvasive optical biopsy by multiphoton microscopy identifies the live morphology of common melanocytic nevi. Pigment Cell Melanoma Res 2020;33:869–77. [PubMed: 32485062]

Levine A, Markowitz O. Introduction to reflectance confocal microscopy and its use in clinical practice. JAAD Case Rep 2018;4:1014–23. [PubMed: 30456275]

Lin J, Saknite I, Valdebran M, Balu M, Lentsch G, Williams JN, et al. Feature characterization of scarring and non-scarring types of alopecia by multiphoton microscopy. Lasers Surg Med 2019;51:95–103. [PubMed: 30248187]

Malvehy J, Alarcon I, Montoya J, Rodríguez-Azeredo R, Puig S. Treatment monitoring of 0.5% 5-fluorouracil and 10% salicylic acid in clinical and subclinical actinic keratoses with the combination of optical coherence tomography and reflectance confocal microscopy. J Eur Acad Dermatol Venereol 2016;30:258–65. [PubMed: 26538346]

Monnier J, De Carvalho N, Harris U, Garfinkel J, Saud A, Navarrete-Dechent C, et al. Combined reflectance confocal microscopy and optical coherence tomography to improve the diagnosis of equivocal lesions for basal cell carcinoma [e-pub ahead of print]. J Am Acad Dermatol 2021. 10.1016/j.jaad.2021.03.066 (accessed February 10, 2022).

Navarrete-Dechent C, Liopyris K, Monnier J, Aleissa S, Boyce LM, Longo C, et al. Reflectance confocal microscopy terminology glossary for melanocytic skin lesions: a systematic review. J Am Acad Dermatol 2021;84:102–19. [PubMed: 32454102]

Nwaneshiudu A, Kuschal C, Sakamoto FH, Anderson RR, Schwarzenberger K, Young RC. Introduction to confocal microscopy. J Invest Dermatol 2012;132:e3. [PubMed: 23187113]

Obeidy P, Tong PL, Weninger W. Research techniques Made Simple: two-photon intravital imaging of the skin. J Invest Dermatol 2018;138:720–5. [PubMed: 29579452]

Olsen J, Holmes J, Jemec GB. Advances in optical coherence tomography in dermatology-a review. J Biomed Opt 2018;23:1–10.

Pezzini C, Kaleci S, Chester J, Farnetani F, Longo C, Pellacani G. Reflectance confocal microscopy diagnostic accuracy for malignant melanoma in different clinical settings: systematic review and meta-analysis. J Eur Acad Dermatol Venereol 2020;34:2268–79. [PubMed: 31997465]

Pouli D, Balu M, Alonzo CA, Liu Z, Quinn KP, Rius-Diaz F, et al. Imaging mitochondrial dynamics in human skin reveals depth-dependent hypoxia and malignant potential for diagnosis. Sci Transl Med 2016;8:367ra169.

Puschmann S, Rahn CD, Wenck H, Gallinat S, Fischer F. Approach to quantify human dermal skin aging using multiphoton laser scanning microscopy. J Biomed Opt 2012;17:036005. [PubMed: 22502563]

Que SKT. Research Techniques Made Simple: noninvasive imaging technologies for the delineation of basal cell carcinomas. J Invest Dermatol 2016;136:e33–8. [PubMed: 27012561]

Sahu A, Yélamos O, Iftimia N, Cordova M, Alessi-Fox C, Gill M, et al. Evaluation of a combined reflectance confocal microscopy-optical coherence tomography device for detection and depth assessment of basal cell carcinoma. JAMA Dermatol 2018;154:1175–83. [PubMed: 30140851]

Saknite I, Zhao Z, Patrinely JR, Byrne M, Jagasia M, Tkaczyk ER. Individual cell motion in healthy human skin microvasculature by reflectance confocal video microscopy. Microcirculation 2020;27:e12621. [PubMed: 32304109]

Sinx KAE, van Loo E, Tonk EHJ, Kelleners-Smeets NWJ, Winnepenninckx VJL, Nelemans PJ, et al. Optical coherence tomography for noninvasive diagnosis and subtyping of basal cell carcinoma: a prospective cohort study. J Invest Dermatol 2020;140:1962–7. [PubMed: 32147505]

Tancrède-Bohin E, Baldeweck T, Brizion S, Decencière E, Victorin S, Ngo B, et al. In vivo multiphoton imaging for non-invasive time course assessment of retinoids effects on human skin. Skin Res Technol 2020;26:794–803. [PubMed: 32713074]

Tkaczyk E. Innovations and developments in dermatologic non-invasive optical imaging and potential clinical applications. Acta Derm Venereol 2017;Suppl 218:5–13.

Vivosight. OCT training, https://vivosight.com/training/; (accessed 19 October 2021).

Wang JY, Wang YJ, Wu YH. In vivo characterization of extramammary Paget's disease by ultra-high cellular resolution optical coherence tomography. Skin Res Technol 2021;27:114–7. [PubMed: 32767528]

Yélamos O, Hibler BP, Cordova M, Hollmann TJ, Kose K, Marchetti MA, et al. Handheld reflectance confocal microscopy for the detection of recurrent extramammary Paget disease. JAMA Dermatol 2017;153:689–93. [PubMed: 28492924]

SUMMARY POINTS

What information optical coherence tomography, reflectance confocal microscopy, and multiphoton microscopy techniques provide

- Optical coherence tomography (OCT): Provides information on overall skin structure (epidermis, dermal–epidermal junction, and papillary and reticular dermis), blood vessels, and hair follicles.
- Reflectance confocal microscopy (RCM): Provides information on cellular structures of the epidermis and dermis, fibrillar structures of the papillary dermis, and microcirculation.
- Multiphoton microscopy (MPM): Provides information on cellular structures of the epidermis and dermis, collagen and elastin of the papillary dermis, and metabolic changes.

Benefits of the OCT, RCM, and MPM

- OCT: deep imaging penetration, large scanning area, and fast imaging.
- RCM: subcellular lateral spatial resolution and large scanning area.
- MPM: submicron lateral spatial resolution and molecular contrast.

Limitations of OCT, RCM, and MPM

- OCT: limited spatial resolution
- RCM: limited contrast
- MPM: limited scanning area

What are OCT, RCM, and MPM clinical devices mostly used for currently?

- OCT: clinical diagnosis of nonmelanoma skin cancers and vascular skin conditions; clinical research.
- RCM: clinical diagnosis of melanoma and nonmelanoma skin cancers; clinical research
- MPM: clinical research

MULTIPLE CHOICE QUESTIONS

1. What skin conditions can be best assessed by optical coherence tomography (OCT)?

- **A.** Melanoma
- **B.** Vascular skin conditions
- **C.** Basal cell carcinoma

2. What skin conditions can be best assessed by reflectance confocal microscopy (RCM) and multiphoton microscopy (MPM)?

- **A.** Melanoma
- **B.** Melanocytic nevi
- **C.** Vascular skin conditions

3. What imaging technologies should be used for visualizing an upward migration of melanocytes?

- **A.** MPM
- **B.** OCT
- **C.** RCM

4. What are the combinations of imaging technologies for the best noninvasive assessment of basal cell carcinoma lesions?

- **A.** MPM and RCM
- **B.** OCT and MPM
- **C.** RCM and OCT

5. What are the common benefits of OCT-, RCM-, and MPM-based devices for clinical skin imaging?

- **A.** Label-free imaging
- **B.** Noninvasive imaging
- **C.** Subcellular resolution

DETAILED ANSWERS

What skin conditions can be best assessed by optical coherence tomography (OCT)?

CORRECT ANSWER: B. Vascular skin conditions; C. Basal cell carcinoma.

Optical coherence tomography (OCT) does not have sufficient spatial resolution for assessing the changes at the cellular level in melanoma.

What skin conditions can be best assessed by reflectance confocal microscopy (RCM) and multiphoton microscopy (MPM)?

CORRECT ANSWER: A. Melanoma; B. Melanocytic nevi

Multiphoton microscopy (MPM) and reflectance confocal microscopy (RCM) have sufficient spatial resolution to capture morphological cellular changes in lesions such as melanocytic nevi and melanoma. OCT is better at assessing vascular skin conditions because it has the ability to capture the morphology of the blood vessel's structure.

What imaging technologies should be used for visualizing an upward migration of melanocytes?

CORRECT ANSWER: A. MPM; C. RCM

MPM and RCM have sufficient spatial resolution to capture an upward migration of melanocytes.

What are the combinations of imaging technologies for the best noninvasive assessment of basal cell carcinoma lesions?

CORRECT ANSWER: B. OCT and MPM; C. RCM and OCT

OCT combined with either RCM or MPM would provide the best assessment of basal cell carcinoma (BCC) because OCT captures the overall morphology, whereas RCM and MPM can resolve the cellular structure inside the BCC nests.

What are the common benefits of OCT-, RCM-, and MPM-based devices for clinical skin imaging?

CORRECT ANSWER: A. Label-free imaging; B. Noninvasive imaging

All the three technologies provide noninvasive, label-free imaging. Only RCM and MPM can generate images with subcellular resolution.

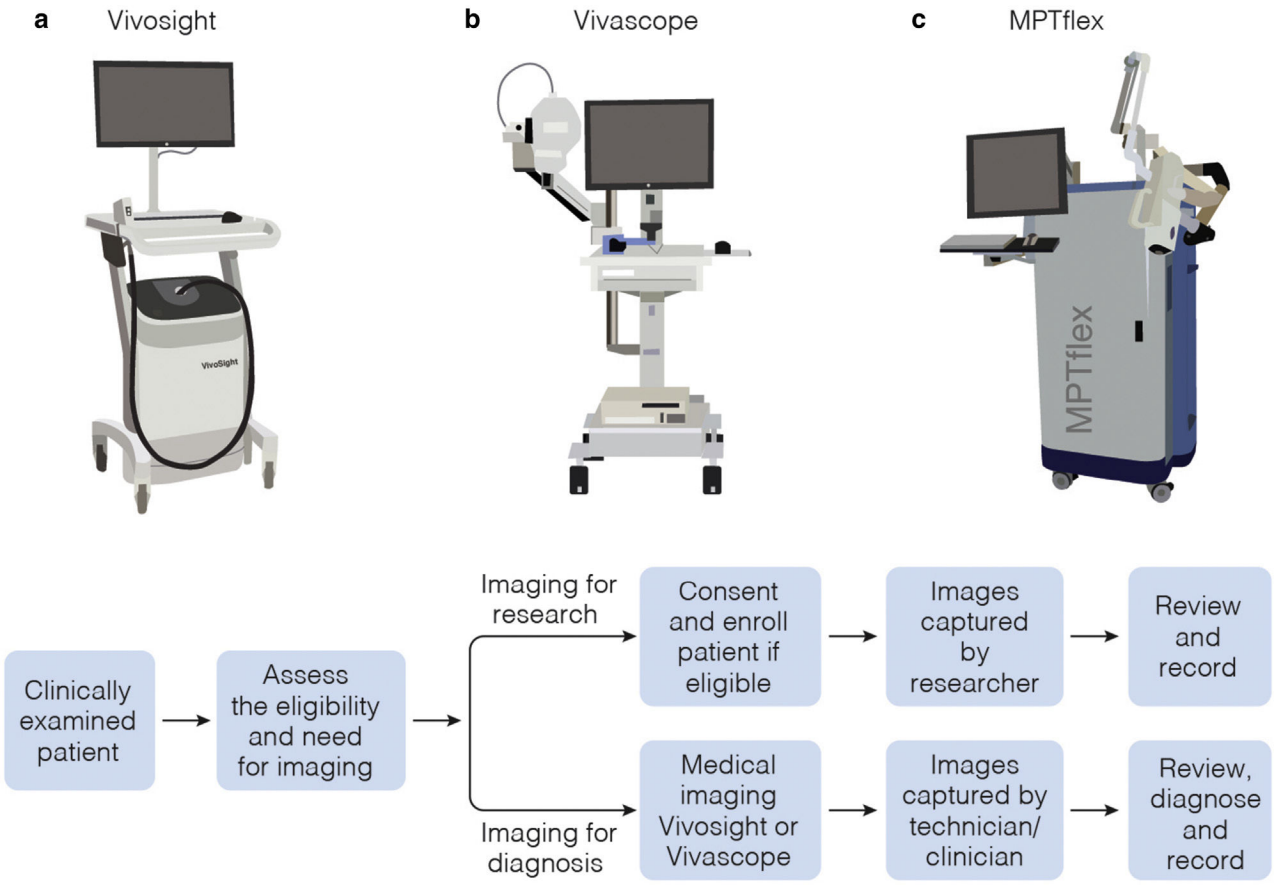

Figure 1. Commercial clinical imaging systems for optical skin biopsy.

(**a**) OCT-based VivoSight (Michelson Diagnostics, Orpington, United Kingdom). (**b**) RCM-based clinical tomograph (VivaScope, CALIBER I.D., Rochester, NY). (**c**) MPM-based clinical tomograph (MPTflex, JenLab GmbH, Jena, Germany). MPM, multiphoton microscopy; OCT, optical coherence tomography; RCM, reflectance confocal microscopy.

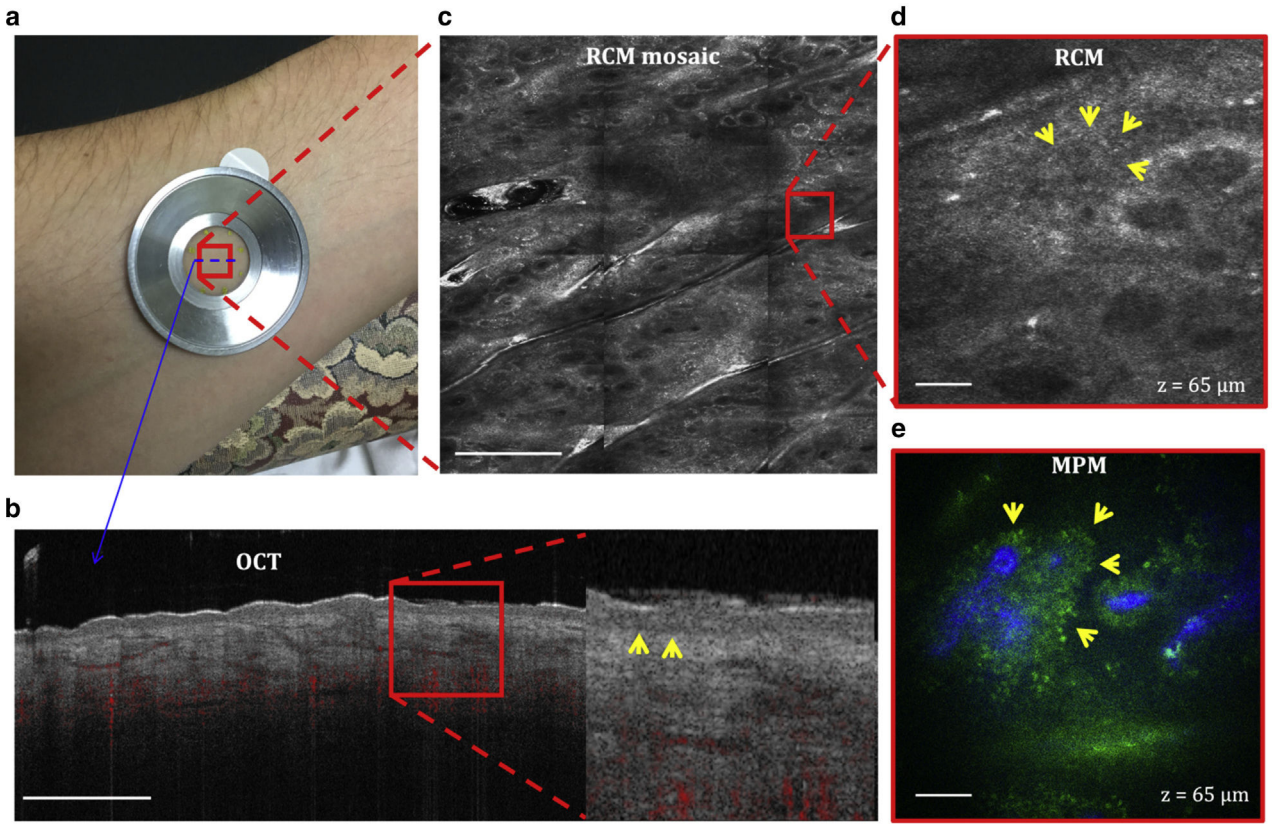

Figure 2. Normal skin.

(**a**) Imaging location on the volar forearm of a volunteer. All the three devices use a metallic ring that attaches to the skin by double-sided tape and to the instrument imaging head magnetically to ensure image stability. (**b**) Cross-sectional (B-scan) OCT image of the skin showing the ability to capture the dermal vascular network (red) and to differentiate the epidermal from the dermal layer by clearly identifying the basal membrane (arrows in the close-up image). Bar = 1 mm. (**c**) Enface (horizontal) RCM mosaic (mm-scale) image showing the overall morphology of the skin at a depth of 65 µm (DEJ). Bar = 500 µm. (**d**) Close-up view of the area outlined in the RCM image in **c** revealing the keratinocytes of the basal layer surrounding the dermal papilla (arrows). Bar = 40 µm. (**e**) Enface MPM image acquired at the same depth showing a similar morphology with the RCM image but with enhanced contrast that clearly distinguishes the dermal papilla collagen (blue) from the surrounding keratinocytes (green, arrows). Bar = 40 µm. DEJ, dermal–epidermal junction; MPM, multiphoton microscopy; OCT, optical coherence tomography; RCM, reflectance confocal microscopy.

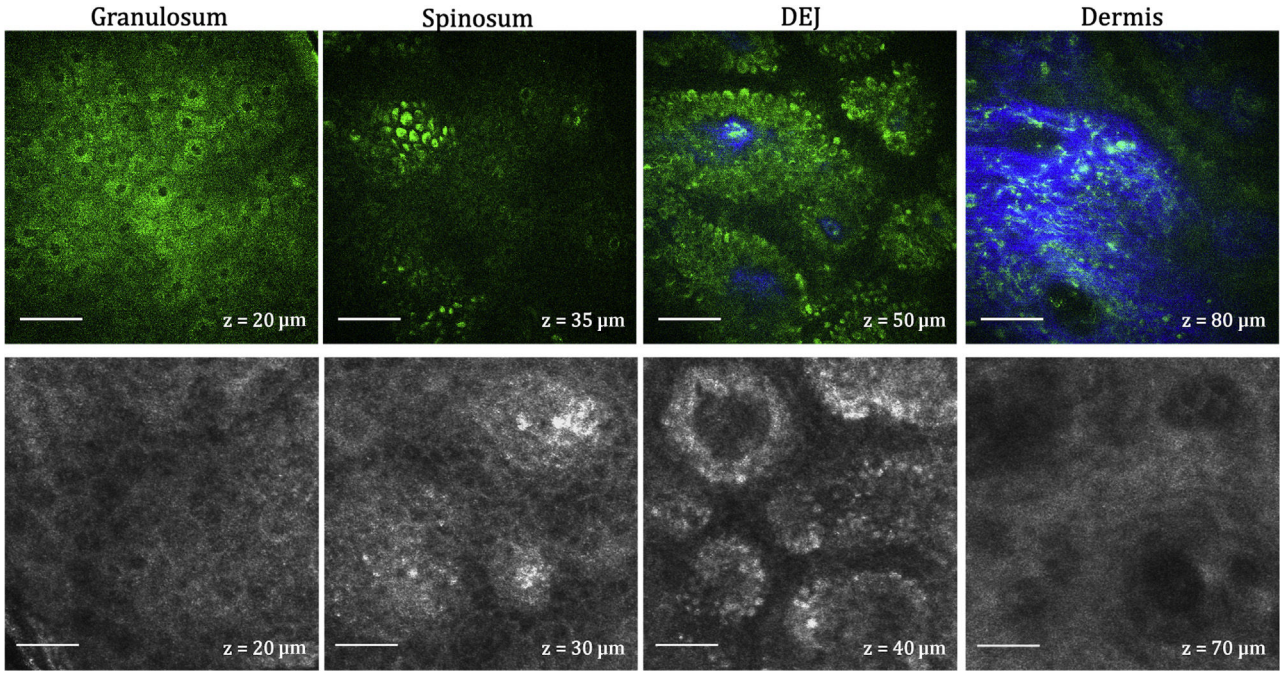

Figure 3. MPM and RCM depth-resolved images of normal skin.

MPM (top) and RCM (bottom) images acquired as z-stacks at different depths from the same location of a volunteer's forearm. The images show the normal architecture of live skin tissue with normally distributed keratinocytes in the granulosum, spinosum, and DEJ layers. Collagen (blue) and elastin (green) fibers are clearly distinguished in the MPM images. Bar = 40 µm in all images. DEJ, dermal–epidermal junction; MPM, multiphoton microscopy; RCM, reflectance confocal microscopy.

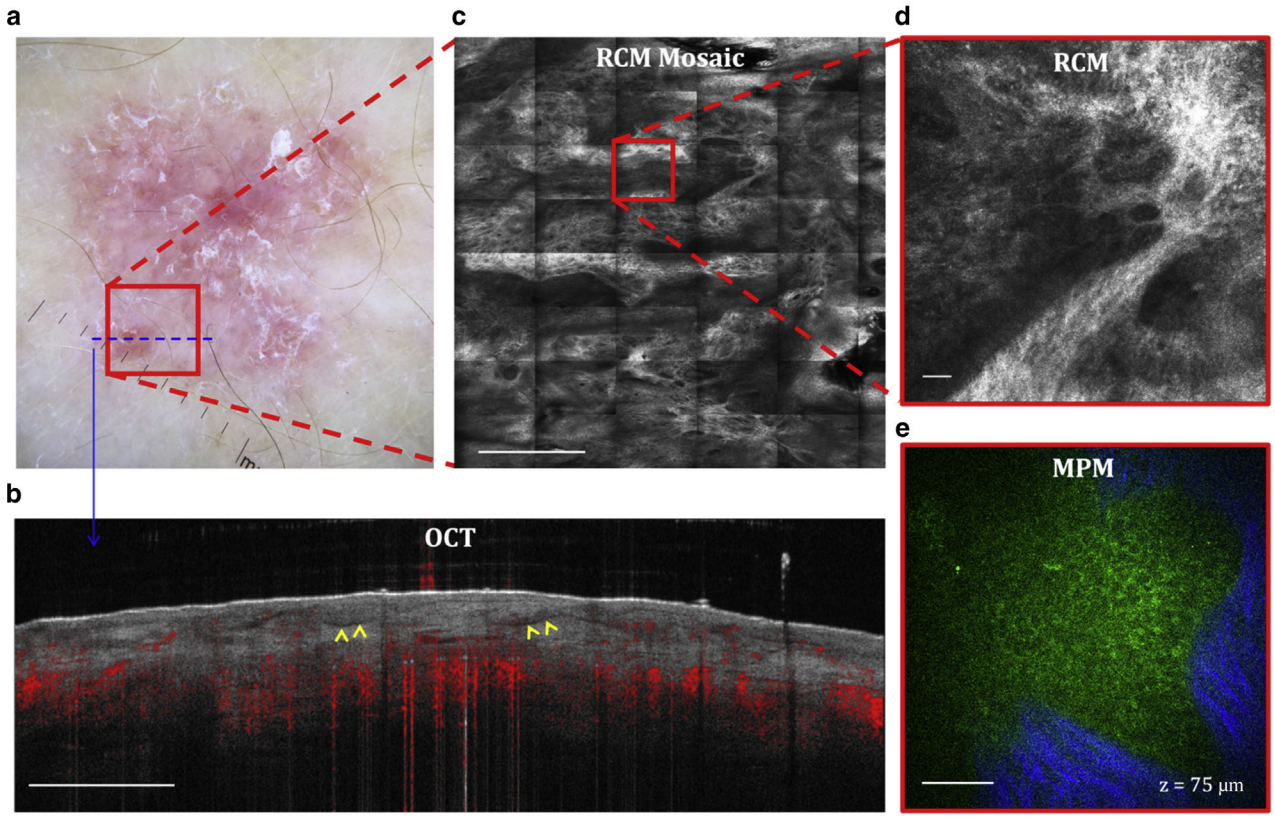

Figure 4. BCC.

(**a**) Clinical image (DermLite FOTO, DermLite, San Juan Capistrano, CA). The outline marker indicates the imaging location. (**b**) Cross-sectional OCT image showing the ability to visualize the BCC nests (arrows). Bar = 1 mm. (**c**) Enface (horizontal) RCM mosaic (mm-scale) image showing the overall morphology of the lesion at a depth of 75 µm (DEJ). Bar = 500 µm. (**d**) Close-up view of the area outlined in the RCM image in c revealing a nest of basaloid cells surrounded by fibrillar structure. Bar = 40 µm. (**e**) Enface MPM image acquired at the same depth showing a nest of basaloid cells (green) surrounded by collagen fibers (blue). Bar = 40 µm. BCC, basal cell carcinoma; DEJ, dermal–epidermal junction; MPM, multiphoton microscopy; OCT, optical coherence tomography; RCM, reflectance confocal microscopy.

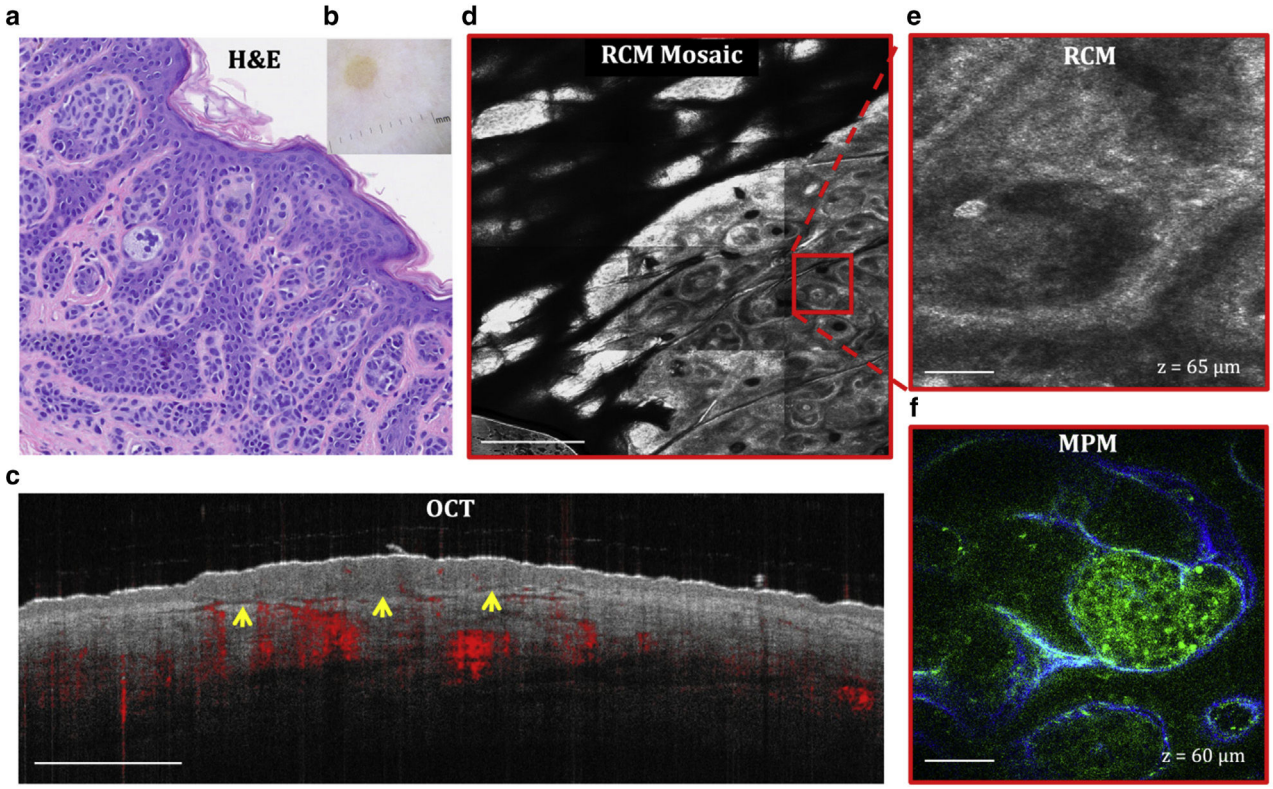

Figure 5. Dermal melanocytic nevus.

(**a**) H&E and (**b**) clinical images of the lesion. (**c**) Cross-sectional OCT image showing the delineation of the lesion depth (arrows). Bar = 1 mm. (**d**) Enface (horizontal) RCM mosaic (mm-scale) image showing the overall morphology of the lesion at a depth of 65 µm (DEJ). Bar = 500 µm. (**e**) Close-up view of the area outlined in the RCM image in **c** revealing the nests of nevus cells surrounded by fibrillar structures. Bar = 40 µm. (**f**) Enface MPM image acquired at the same depth showing the nests of nevus cells (green) surrounded by collagen fibers (blue). Bar = 40 µm. DEJ, dermal–epidermal junction; MPM, multiphoton microscopy; OCT, optical coherence tomography; RCM, reflectance confocal microscopy.

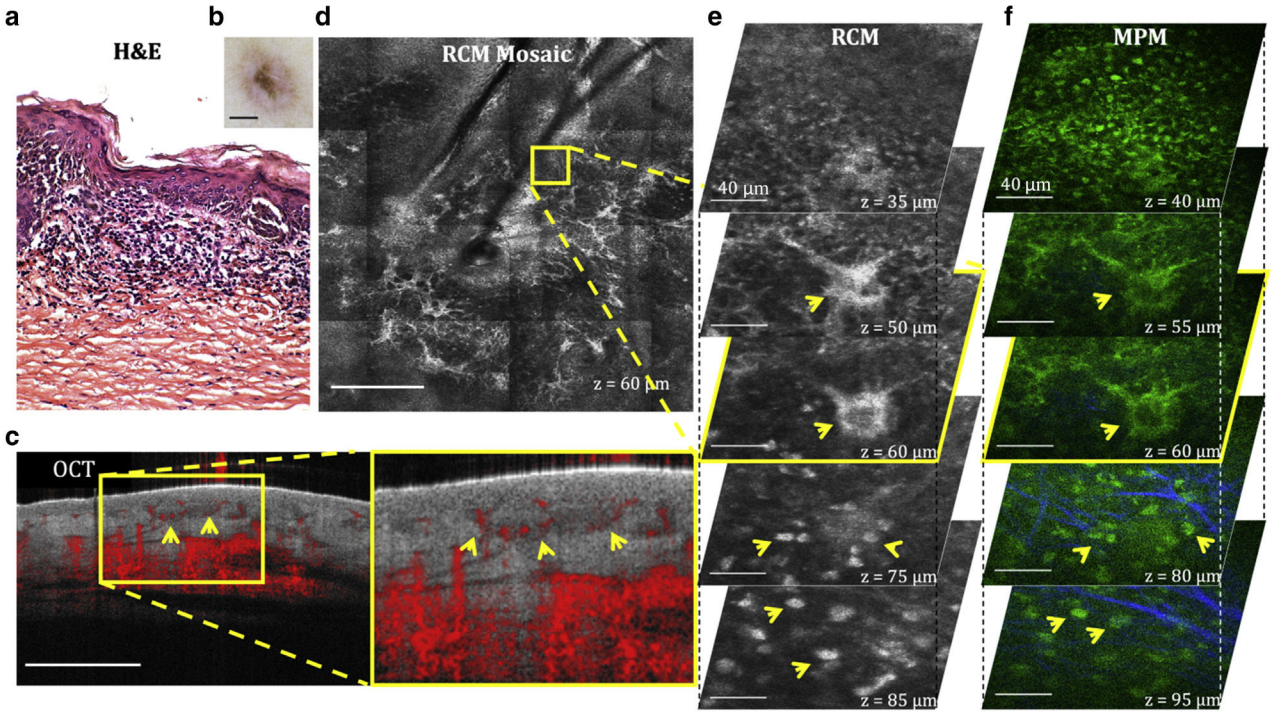

Figure 6. Recurrent melanocytic nevus.

(**a**) H&E and (**b**) clinical images of the lesion. (**c**) Cross-sectional OCT image showing the delineation of the lesion depth with relatively low contrast (arrows). Bar = 1 mm. (**d**) Enface (horizontal) RCM mosaic (mm-scale) image showing the overall morphology of the lesion at a depth of 60 µm (DEJ). Bar = 500 µm. (**e**) 3D RCM images enclosing the area outlined in the RCM image in **d**, revealing dendritic cells (arrows) in the basal layer (z = 50 µm, 60 µm) and nests of inflammatory cells (arrows, z = 75 µm, 85 µm) surrounded by fibrillar structures. Bar = 40 µm. (**f**) 3D MPM images acquired at the same location showing the dendritic cells (arrows) in the basal layer (z = 40 µm, 55 µm) and nests of inflammatory cells (arrows, z = 80 µm, 95 µm) surrounded by collagen fibers (blue). Bar = 40 µm. 3D, three-dimensional; DEJ, dermal–epidermal junction; MPM, multiphoton microscopy; OCT, optical coherence tomography; RCM, reflectance confocal microscopy.

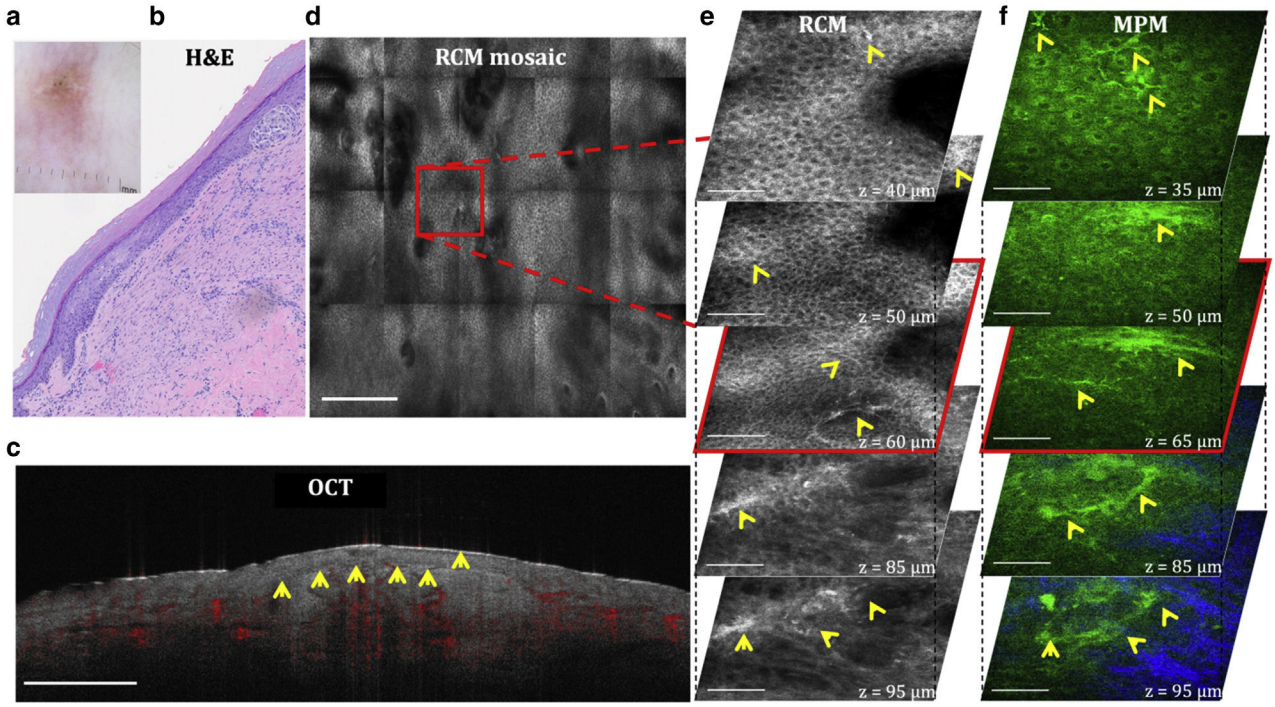

Figure 7. Residual/recurrent nevus with a previous diagnosis of Spitz nevus.

(**a**) Clinical and (**b**) H&E images of the lesion. (**c**) Cross-sectional OCT image showing the delineation of the lesion depth with relatively low contrast (arrows). Bar = 1 mm. (**d**) Enface (horizontal) RCM mosaic (mm-scale) image showing the overall morphology of the lesion at a depth of 60 µm (spinosum layer). Bar = 500 µm. (**e**) 3D RCM images enclosing the area outlined in the RCM image in **d**, revealing the presence of dendritic cells (arrows) in the spinosum (z = 40 µm, 50 µm) and basal (z = 60 µm) layers and a nest of dendritic cells at the DEJ (z = 85 µm, 95 µm). Bar = 80 µm. (**f**) 3D MPM images acquired at the same location, showing the presence of dendritic cells (arrows) at similar depths as those of RCM and a nest of dendritic cells clearly delineated by collagen fibers (blue). Bar = 40 µm. 3D, three-dimensional; DEJ, dermal–epidermal junction; MPM, multiphoton microscopy; OCT, optical coherence tomography; RCM, reflectance confocal microscopy.

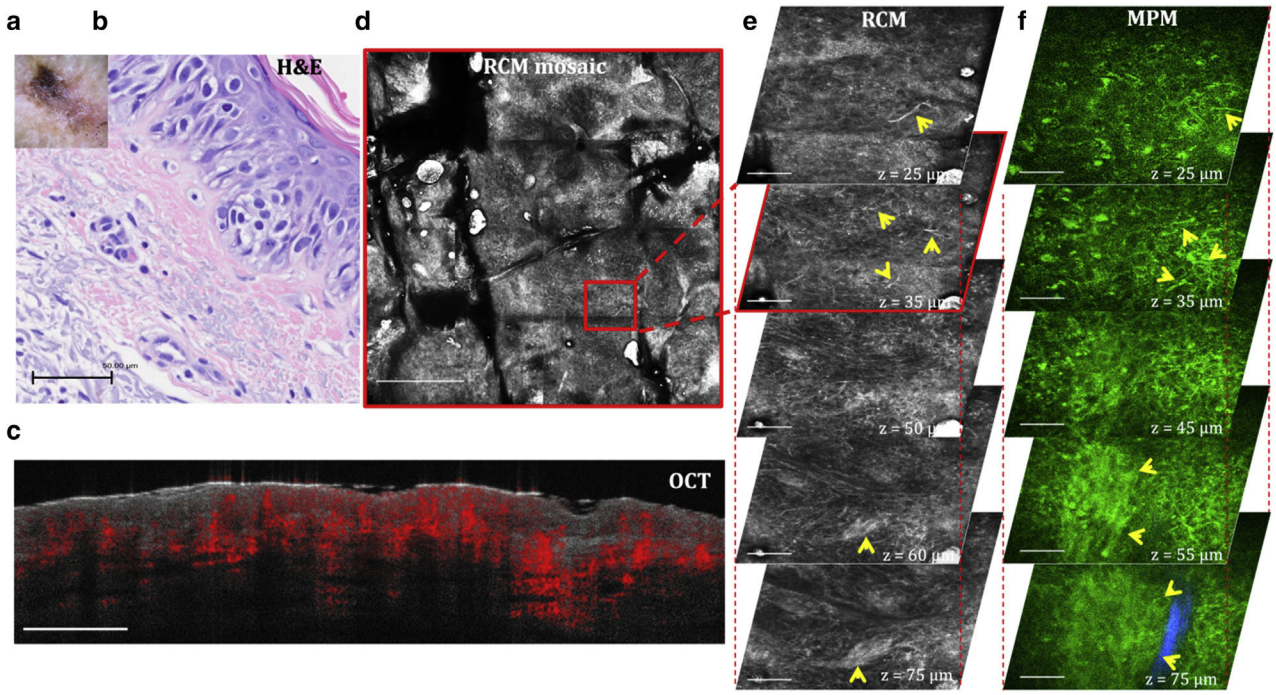

Figure 8. Melanoma.

(**a**) Clinical and (**b**) H&E images of the lesion. (**c**) Cross-sectional OCT image showing a raised lesion with increased density of blood vessels. Bar = 1 mm. (**d**) Enface (horizontal) RCM mosaic (mm-scale) image showing the overall morphology of the lesion at a depth of 35 µm (spinosum layer). Bar = 500 µm. (**e**) 3D RCM images enclosing the area outlined in the RCM image in **d**, revealing migrating melanocytes in the spinosum layer (arrowheads, z = 25 µm, 35 µm), epidermal disarray (z = 25–75 µm), and nests of melanoma cells at the DEJ (arrowheads, z = 75 µm). Bar = 100 µm. (**f**) 3D MPM images acquired at the same location showing migrating melanocytes in the spinosum layer (arrowheads, z = 25 µm, 35 µm), epidermal disarray (z = 25–75 µm), and a nest of melanoma cells (arrowheads) surrounded by collagen fibers (blue) at the DEJ (z = 75 µm). Bar = 40 µm. 3D, three-dimensional; DEJ, dermal–epidermal junction; MPM, multiphoton microscopy; OCT, optical coherence tomography; RCM, reflectance confocal microscopy.

Table 1.

Optical Imaging Technologies for Noninvasive Optical Skin Biopsy: Key Parameters

Optical Imaging System/Key Parameters	MultiBeam OCT (VivoSight)	RCM (VivaScope)	MPM (MPTflex)
Contrast	Scattering	Scattering	TPEF/SHG
Lateral spatial resolution	<7.5 μm	~1 μm	<1 μm
Axial spatial resolution	<5 μm	<2 μm	<2 μm
Imaging depth	<2 μm	<250 μm	<250 μm
Imaging FOV	6 × 6 mm^2	500 × 500 μm^2 (single image) up to 8 × 8 mm^2 (tiling) [1]	250 × 250 μm^2 (single image)
Imaging time per unit area	0.02 s/mm^2	0.5 s/mm^2	96 s/mm^2
Estimated total imaging time	few seconds	Tens of seconds to a few minutes	10–20 minutes
Key performance features	Deep penetration Large FOV	Subcellular resolution + large FOV	Submicron resolution Molecular contrast
Limitations	Low spatial resolution No molecular contrast	No molecular contrast	Limited FOV
Clinical value for skin imaging	3D macroscopic view of the lesion morphology	Macroscopic view of the lesion morphology with subcellular resolution	Selective visualization of the cellular and extracellular matrix with submicron resolution
Morphological features visualized in BCC, recurrent nevi, and melanoma	BCC nests Overall 3D delineation of lesions	BCC nests, dendritic and immune cells, melanocytes, and overall cellular and fibrillar structure	Cellular-resolved BCC and nevus cell nests, dendritic and immune cells, melanocytes, and collagen and elastin fibers

Abbreviations: 3D, three-dimensional; BCC, basal cell carcinoma; CPT, Current Procedural Terminology; FOV, field ofview; MPM, multiphoton microscopy; OCT, optical coherence tomography; RCM, reflectance confocal microscopy; SHG, second harmonic generation; TPEF, two-photon excited fluorescence.

[1] The handheld version of the RCM clinical device (VivaScope 3000) can scan a larger area, but it is not currently covered by the CPT I codes.